THESIS FOR THE DEGREE OF LICENTIATE OF ENGINEERING

Axial Mixing of Large Solids in Fluidised Beds – Modelling and Experiments

ANNA KÖHLER

Department of Space, Earth and Environment

CHALMERS UNIVERSITY OF TECHNOLOGY

Gothenburg, Sweden 2019

Axial Mixing of Large Solids in Fluidised Beds – Modelling and Experiments

ANNA KÖHLER

© ANNA KÖHLER, 2019.

Department of Space, Earth and Environment
Chalmers University of Technology
SE-412 96 Gothenburg
Sweden
Telephone + 46 (0)31-772 1000

Printed by Chalmers Reproservice
Chalmers University of Technology
Gothenburg, Sweden 2019

Axial Mixing of Large Solids in Fluidised Beds
– Modelling and Experiments

ANNA KÖHLER
Division of Energy Technology
Department of Space, Earth and Environment
Chalmers University of Technology

Abstract

Fluidisation is a technology commonly found wherever particulate solids are to be transported, mixed and/or reacted with a gas. At present, it is a widespread technology with applications ranging from the production of carbon nanotubes in the manufacturing industry to the conversion of solid fuels in the heat and power sector. As for the latter, fluidised beds are well received for their fuel flexibility (being able to efficiently convert low-grade fuels) and for their ability to control emissions with in-bed methods. In most applications, like solid fuel conversion, the heat and mass transfer between the gas and the solids (e.g. fuel particles) play an important role in the process performance. In turn, these transfer mechanisms are affected by the axial solids mixing, as solids immersed in the dense bed will experience higher heat transfer and lower mass transfer than otherwise.

This work focuses on the axial mixing of large solids in fluidised beds with the aim to advance current knowledge on in-bed mixing with an emphasis on biomass particles. As the latter typically have a high content of moisture, volatile and ash and are larger and lighter than conventional fuels like e.g. coal or lignite, they are even more prone to segregate axially in the bed in a flotsam fashion. Yet, the effect of fuel density and size as well as the effect of fluidisation conditions on the axial mixing of fuel has not been fully understood.

To enhance the understanding of solids mixing, this work combines a one-dimensional semi-empirical model with experiments applying magnetic particle tracking (MPT) in a fluid-dynamically down-scaled fluidised bed. The model is used to identify governing mechanisms and the respective key parameters to be studied with dedicated experiments which, in their turn, contribute to the continuous upgrading of the model.

The key parameters in the axial mixing of larger solids in a fluidised bed are found to be: i) the apparent viscosity of the emulsion, for which MPT measurements confirmed its Newtonian character, and ii) the bubble flow, which experiments revealed to have a higher upwards velocity and fuel-to-bubble velocity ratio than shown in previous literature not accounting for hot conditions.

Keywords: fluidised beds, solids mixing, semi-empirical modelling, fluid-dynamic down-scaling, magnetic particle tracking

List of publications

This thesis is based on the work presented in the following publications, which are referred to in the text by their Roman numerals:

Paper I	Anna Köhler, David Pallarès and Filip Johnsson. Modelling Axial Mixing of Fuel Particles in the Dense Region of a Fluidised Bed. *To be submitted.*
Paper II	Anna Köhler, David Pallarès and Filip Johnsson. Magnetic tracking of a fuel particle in a fluid-dynamically down-scaled fluidised bed. Fuel Processing Technology, 2017, Volume 162, 147-156
Paper III	Anna Köhler, Alexander Rasch, David Pallarès and Filip Johnsson. Experimental characterization of axial fuel mixing in fluidized beds by magnetic particle tracking. Powder Technology, 2017, Volume 316, 492-499
Paper IV	Anna Köhler, David Pallarès and Filip Johnsson. Determination of the Apparent Viscosity of Dense Gas-Solids Emulsion by Magnetic Particle Tracking. 23rd International Conference on Fluidized Bed Conversion, Seoul, Korea, 2018

Contributions of the authors

Anna Köhler is the principal author of the Papers I–IV and was the main responsible of the modelling work and data processing of Paper I and the experimental work and data analysis of Paper II and IV. For the work of Paper III, she was responsible of the setup of the experimental work and main responsible of the data analysis.

Associate Professor David Pallarès has contributed with ideas regarding the design of the model and the experiments, discussions and guidance, and with the editing of all four papers.

Professor Filip Johnsson has contributed with discussions, and guidance, as well as the editing of all four papers.

Alexander Rasch has conducted the experiments and contributed to the data analysis of Paper III.

Additional publications related to the work are listed below but have not been included in the thesis as they are either outside the scope of the thesis or overlap with the appended articles.

1) Erik Sette, Anna Köhler, David Pallarès and Filip Johnsson.
   3-dimensional particle tracking in a fluid-dynamically downscaled fluidized bed using magneto resistive sensors.
   The 8th International Symposium on Coal Combustion, Beijing, China, 2015
2) Anna Köhler, David Pallarès and Filip Johnsson.
   Modelling Axial Mixing of Char – Application to the Dense Bottom Bed in CFB Boilers.
   12th International Conference on Fluidized Bed Technology, Krakow, Poland, 2017

Acknowledgements

Pursuing a PhD is an adventurous – at times troublesome – journey, which couldn’t be walked alone. This is to acknowledge the ones, who were with me on my journey.

Henrik, thank you for your enthusiasm and ideas always giving my work a wider perspective. Filip, I’m very grateful for your input and your interest in my work. No matter how unreasonable the timeframe, your positive manner and comprehensive feedback are assured, which make it a pleasure to work with you.

David, I really enjoy our numberless discussions, which pave the way of my development both as a researcher and as a person. Your visualisations simplifying complex problems scribbled on a piece of paper have been invaluable – like ‘treasure maps’ to me, guiding through the next leg of my journey. Thank you for your trust and your support, I can always rely on.

I would like to thank Youngdoo, Jessica, Ulf and Rustan, who were involved in the experimental part of my work. Rustan, your structured and creative way of solving technical problems in the lab are worth a mint for a lost PhD student. Bo, although reading in Russian is still not an option for me, I’m glad to have your guidance through the deep jungle of literature.

Dear colleagues, what would Energy technology be without you? Thank you, Max, for all the chats over real espresso and being a lovely friend; Adrian, for bearing to share an office with me; Viktor, Sebastien, Tove, Angelica and Guillermo – because it’s more fun to travel together; all you from the thermo-gang, it’s a great pleasure to work with you. A special thanks goes to the one and only A-team for all the help I got from you since I started at the division.

To my friends and family in Germany and Switzerland, I’m very grateful to have you in my life. You are missing here. To my Swedish family, thank you for making me feel like home in this weather-worn country. And to my dear Anders, thank you for always being with me on this journey. On the rocky road of life, I cannot think of something better than feeling my hand in yours, when walking side by side with you.

This work has been financed by the Swedish Gasification Centre (SFC) within the framework of the Centre for Indirect Gasification of Biomass (CIGB).

Anna Köhler
Hong Kong, May 2019

Table of Contents

Abstract III
List of publications V
Acknowledgements VII
1 Introduction 1
  1.1 Aims and Scope 3
  1.2 Fluidisation, Bubbles and Solids Mixing 3
  1.3 Structure of the Thesis 6
2 Modelling Work 9
3 Experimental Work 11
  3.1 Fluid-dynamically down-scaled fluidised bed 11
  3.2 Magnetic particle tracking 12
  3.3 Falling sphere experiments 13
4 Results and Discussion 15
  4.1 Combination of modelling and experimental work 15
  4.2 Axial mixing of large solids 19
5 Conclusions 23
6 Future research 25
Notation 27
References 29

1 Introduction

Fluidisation is the dynamic fluid-like state that develops as gas passes through a bed of particulate solids. Originally developed for the gasification of coal in the 1920s through the Winkler process, fluidisation is now a widely used technology. Fluidised bed (FB) units can be found in all kinds of applications, ranging from particle classification, pneumatic transport, filtration, and drying and coating over different catalytic processes in the petrochemical industry to the conversion of solid fuels in combustion and gasification processes [1]. New applications, such as the production of carbon nanotubes [2] and chemical looping combustion to capture the greenhouse gas CO_2 [3], have been added to the list in the past few years. What all these processes have in common is the need to transport and/or mix particulate solids frequently, with special emphasis on the transfer of heat and mass with the fluidising gas.

The largest FBs are used for the combustion of solid fuels with dimensions of medium-sized multi-storey buildings, while the particulate solids used in the beds are as small as fine grains of sand. Besides the gas phase in the form of bubbles, various types of solids may be present in the bed, including bulk solids (fuel ashes, sand and/or active bed materials, such as oxygen carriers, catalysts and sorbents) and fuel particles (e.g., biomass, waste, plastics, peat, coal). The latter particles are typically larger and lighter than the bed material. Momentum, heat and mass are exchanged within and between all the phases over a wide range of length and time scales, which means that fluidised beds are complex multiphase flow systems and that performing modelling and measurements is a challenging task [4].

In the early stages of development, scarce knowledge and limited computational capacity [5] made the use of experimental correlations the main tool for optimising the design and operation of fluidised beds. As knowledge has expanded and computational power has increased, the tools for extrapolative design and operation and the modelling of FB units have been developed. In general, there are two types of models: computational fluid dynamics (CFD) and semi-empirical modelling. CFD, which is derived from first principles, provides solutions to generic, governing equations. However, CFD models present challenges in the forms of high computational cost (e.g., due to the high number of particles in Lagrangian modelling) and uncertainties in terms of the coefficients in the governing equations (e.g., the solid stress tensor for Eulerian representations of the solids phase). Semi-empirical process models usually do not solve the velocity fields of the gas and bulk solids through momentum balances but rather by applying simpler sub-models, assumptions, and data derived from experiments. Thus, these models lack the level of detail of CFD and are somewhat restricted to the range of parameters used during their development, although they can simulate the whole process with affordable computational times (hours), making them a powerful tool for design and engineering purposes [6]–[8].

The FB technology used for the conversion of solid fuels (combustion, gasification) has two main advantages over other technologies (e.g., pulverised fuel units and grate-fired units) [9]. FB systems have high fuel flexibility, with the ability to convert low-grade solid fuels, such as waste and biomass, without the need for extensive fuel preparation, while still enabling stringent control of conversion. Second, FB systems enable in-bed reductions of polluting emissions, such as nitrogen and sulphur oxides, through the addition of sorbents to the bed (and, with modifications, CO_2 capture without a major energy penalty). A critical but sparsely studied phenomenon in FB units for solid fuel conversion is the mixing of the larger and lighter fuel particles in the dense bed of the finer and heavier bulk solids. In particular, the axial mixing of the fuel particles has a direct impact on the rates of fuel conversion and lateral mixing. As for the fuel conversion, fuel floating on the bed surface will result in a lower bed-to-fuel heat transfer rate than fuel that is immersed in the bed [10], and this will entail longer drying and devolatilisation times and may result in a less-reactive char [11]. Furthermore, the char conversion itself for particles floating on the bed surface will occur under lower heat transfer, albeit with better mass transfer of gases to the particle than is the case for char immersed in the bed, conferring faster burnout times for combustion and an uncertain impact on gasification. As for the lateral mixing, fuel that floats on the bed surface will spread faster in the lateral directions than fuel that is immersed in the bed [12]. Rapid lateral mixing of fuel is often desirable to avoid maldistribution of the fuel (and thus, of the gas species and temperature) over the cross-section. However, in units with a cross-flow of bed material, this can lead to insufficiently long residence times for the fuel in the bed.

While research efforts in the past have focused primarily on understanding processes with conventional fuels, such as coal and lignin, current geopolitical and environmental challenges have prompted interest in more local and sustainable fuels, such as biomass and renewable waste fractions. These low-grade fuels typically have high contents of volatiles, often in combination with high moisture contents. As a consequence, they release significant amounts of gas, which provides them with an extra buoyancy force. This, together with their large size and low density, promotes in-bed fuel segregation, which becomes a new important aspect to consider during the design and operation of FB units for solid fuel conversion.

1.1 Aims and Scope

This thesis aims at advancing current knowledge of in-bed mixing, which is crucial for describing the axial mixing of fuel particles in fluidised bed applications. A special focus is on the mixing of biomass particles. While the scope is limited to bubbling fluidised beds, it should be noted that these have previously shown [13] to exhibit an overall flow behaviour that is similar to that of the bottom region (dense bed and splash zone) of fluidised beds operating under circulating conditions.

To understand how the size and density of the fuel, properties of the bed material, and fluidisation conditions affect the vertical distribution of the fuel over the bed height, a semi-empirical, one-dimensional model is combined with experiments. The model provides a mathematical description of the problem and is used to identify the key parameters and knowledge gaps to be investigated in targeted experiments. The experimental work is carried out in a fluid-dynamically down-scaled unit, to provide quantitative relevance to the measurement data, as hot and large-scale conditions are mimicked. Measurements are carried out by magnetic particle tracking (MPT), which enables high temporal and spatial resolutions. The work includes the further development and refinement/tuning of the MPT technique for the performance of measurements in fluid-dynamically down-scaled fluidised beds.

1.2 Fluidisation, Bubbles and Solids Mixing

Fluidisation of a bed of particulate material, which can be divided into several stages (Figure 1.1), is achieved by passing a gas through the particles [14]. At very low gas velocities, the particles remain still in a fixed bed as a preliminary step to fluidisation. When the gas velocity is increased to the minimum fluidisation velocity the particles enter the minimum fluidisation stage, in which the behaviour of the bed resembles that of a fluid, i.e., the bed surface is smooth and the fluid-dynamical properties, such as density and viscosity, can be assessed. When the gas velocity is further increased, gas bubbles form in the bottom of the chamber, move upwards, and eventually erupt at the bed surface. The bed consists then of a bubble phase (typically assumed to be solids-free) and an emulsion phase, which consists of solids and gas and exhibits the same properties as the fluid-like phase at minimum fluidisation [15]. As they ascend, the bed bubbles cause solids displacement patterns and thereby initiate solids mixing. Solids drift along the bubbles' surfaces and are pulled upwards in the wake of the bubbles

[16]–[19]. Finally, when the bubbles erupt at the bed surface, bed material is ejected into the freeboard and scattered in the lateral direction [20]. Thus, bubbles are the main driving force for solids mixing in the dense region of a fluidised bed.

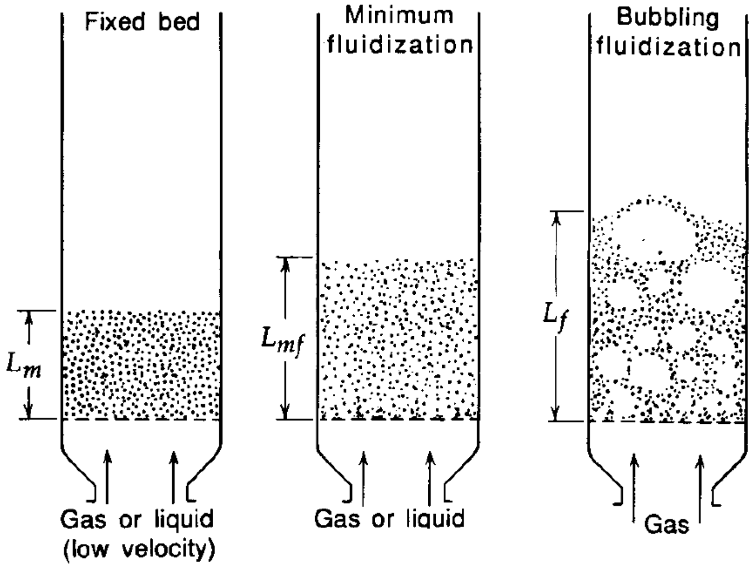

Figure 1.1: Stages of gas fluidisation for a bed of particulate material. Adapted from Kunii and Levenspiel [14].

Historically, the bed has been divided based on gas flows into two phases: the bubble-free zones are the emulsion phase, exhibiting the same properties as the fluid-like phase at minimum fluidisation [15], while the additional gas flow is present in the bubble phase. This classic two-phase theory has been shown to over-predict expansion of the bed and has subsequently expanded with a throughflow, a third gas flow that passes through the bubbles [21].

Furthermore, a portion of the solids is present in the wake of the rising bubbles, suggesting a division into different zones of wake (upwards-rising) and drift (downward-drifting) solids rather than the distinguishing of gas phases. In shallow and wide beds (typical for large-scale conversion of solid fuels), the bubbles form bubble paths [12], [22], [23] – a stream of rising bubbles trailing along roughly the same path – around which the motion of the bed material forms a toroidal pattern (Figure 1.2), known as the ‘gulf stream’ flow pattern [14]. Bed material is dragged upwards in the inner region of the toroid, where bubbles flow and move downwards in the (bubble-free) outer region of the toroid to fulfil the mass balance. Fuel particles are carried along with the solids flow and circulate through the bed in a similar manner. The fuel particle circulation can be divided into axial motion and lateral motion, as indicated in Figure 1.2. The dominating axial motion is characterised by the drag of sinking solids (a) and the drag of rising wake solids (c) on the fuel particle [16], [17], [22]. The lateral motion in the bed is induced by the fuel particle being dragged into a bubble path (b) or by it being released from the latter (d) [16], [24], while lateral mixing on the bed surface is caused by the scattering of bubble eruption (e) [20].

Whether fuel particles mix or segregate axially is mainly a function of their own physical properties, as well as the fluidisation conditions of the bed [25]–[27]. The lower density of the fuel particles relative to the bulk solids makes the former prone to segregate on the bed surface (Figure 1.2, f), while a more vigorous fluidisation results in the axial circulation of bulk solids dragging the fuel particles into the bed, thereby yielding a wider distribution of the fuel over the bed height.

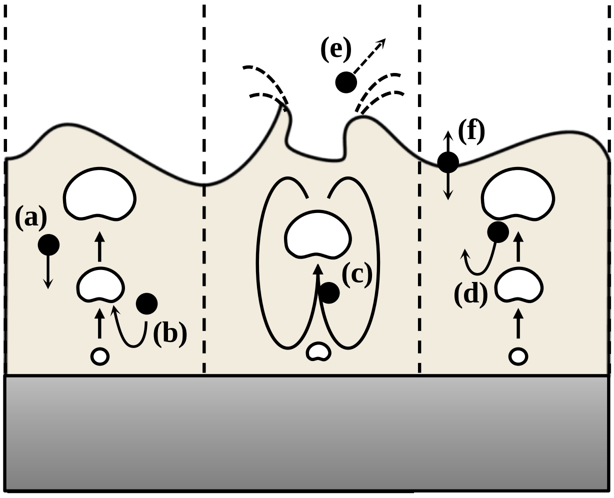

Figure 1.2: Development of bubble paths and the movement of fuel particles in bubbling fluidised beds.

When modelling the mixing of larger solids (i.e., fuel particles) in a fluidised bed, the forces that the gas-solids emulsion (buoyancy and drag) exerts on the object must be assessed. For this purpose, the gas-solids emulsion can be treated as a fluid with fluid-dynamic properties, such as density and viscosity. The emulsion density, ρ_e, plays an important role in the buoyancy and drag forces on an object and can be expressed relatively easily with the bed porosity [14] measuring the pressure difference, Δp along a distance, Δz, in the dense bed [28], here at minimum fluidisation:

$$\rho_e = (1 - \varepsilon_{mf})\rho_s + \varepsilon_{mf} \cdot \rho_g \tag{1}$$

$$\frac{\Delta p}{\Delta z} = (1 - \varepsilon_{mf})(\rho_s - \rho_g) \cdot g \tag{2}$$

The viscosity indicates how much drag the studied particle will experience from the surrounding gas-solids emulsion moving at a certain relative velocity. Viscosity measurements of fluids are often performed in viscosimeters, where the fluids run through a defined capillary tube, a method that is obviously unsuitable for a fluidised bed. Different approaches to measure the viscosity of gas-solids emulsions can be found in the literature, such as investigating the bubble shape [29] or using a Couette viscometer [30]. Another common method is the falling sphere method, where a spherical solid tracer is released into the bed at minimum fluidisation [31]–[35]. By measuring the terminal velocity of the tracer, the drag coefficient can be calculated, which leads to the Reynolds number of the flow and thereafter, the apparent viscosity, μ_e, of the emulsion.

1.3 Structure of the Thesis

To gain a better understanding of axial mixing of large solids in fluidised beds, this work combines two elements: modelling and experimental work (Figure 1.3). The two elements are connected given that the semi-empirical model is fed with data extracted from experiments, while the model serves to identify those key mechanisms that warrant being investigated experimentally.

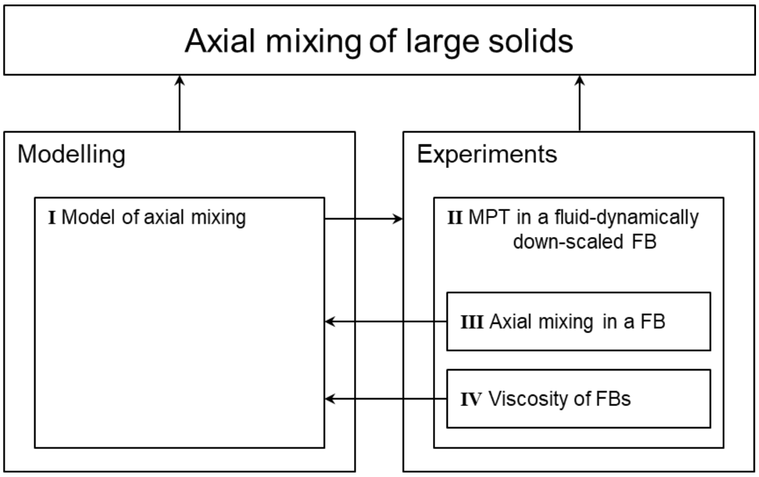

Figure 1.3: Structure of the thesis, including the publications (Papers I–IV): combining modelling with an experimental approach.

This thesis is based on the work presented in the four appended papers. The modelling work, in the form of a 1-dimensional model for the axial mixing of large objects in a fluidised bed, is described in Section 2 and in Paper I. The experimental work is briefly outlined in Section 3 and is described in more detail in Papers II, III and IV.

Paper II presents how MPT can be used in fluid-dynamically down-scaled fluidised beds to investigate the movement of a tracer in all three spatial dimensions and time. The diagnostic technique is evaluated and refined, and both possibilities and limitations are identified.

In Paper III, MPT and fluid-dynamical down-scaling are combined to measure the axial mixing of spherical tracers in bubbling fluidised beds. The experiments cover various tracer densities, bed heights, fluidisation velocities, and pressure drops over the air distributor of the bed. The resulting measurement data represent the main contribution in terms of empirical input to the model presented in Paper I; namely, the probability that the tracer will leave the emulsion zone with the downwards-flowing solids and join the wake solids with the rising bubbles.

Paper IV is a first step towards increasing our understanding of the viscosity of the emulsion phase in fluidised beds. This parameter was, through model runs, identified as a key target for experimental investigations (see *Publications not included in this thesis* above), given its strong impact on the axial mixing of solids and the scarce information in the literature. This paper presents experiments that determine the viscosity of the emulsion at minimum fluidisation by combining the falling sphere method with MPT. The work covers a literature review of the knowledge gained in the past and includes experimental results that provide explanations for the apparently contradictory conclusions in the previous studies. The conclusions drawn are in turn used in the modelling work by applying refined values and expressions for the viscosity of the emulsion.

2 Modelling Work

The dynamic one-dimensional model to simulate the axial mixing of a large particle in a bubbling fluidised bed is set up as Lagrangian tracking system that describes the z-position of a single large particle (Figure 2.1). The model differentiates between the dense bed and the splash zone above it. The dense bed is itself divided into two zones: 1) the bubble wake zone with gas in the form of bubbles, rising at the velocity u_b, and with bed solids flowing upwards in the bubble wakes; and 2) the emulsion zone, which is a bubble-free emulsion of gas flowing upwards at the minimum fluidisation velocity, u_{mf}, and sinking bulk particles. In a bubble-free bed, the particles are held up by the gas flow, whereas in bubbling fluidised beds they sink as they make up for the wake solids that are rising in the bubble wake zone.

The schematic in Figure 2.1 shows how the fuel, mimicked by a single spherical tracer, is tracked through the bed starting in the emulsion zone. In time-steps with the occurrence of a bubble passage, the probability of the particle leaving the zone and starting to rise with the wake solids, q, is applied. These probability values were obtained from experiments ([36], Paper III). Once it reaches the bed surface, the tracer is ejected into the splash zone.

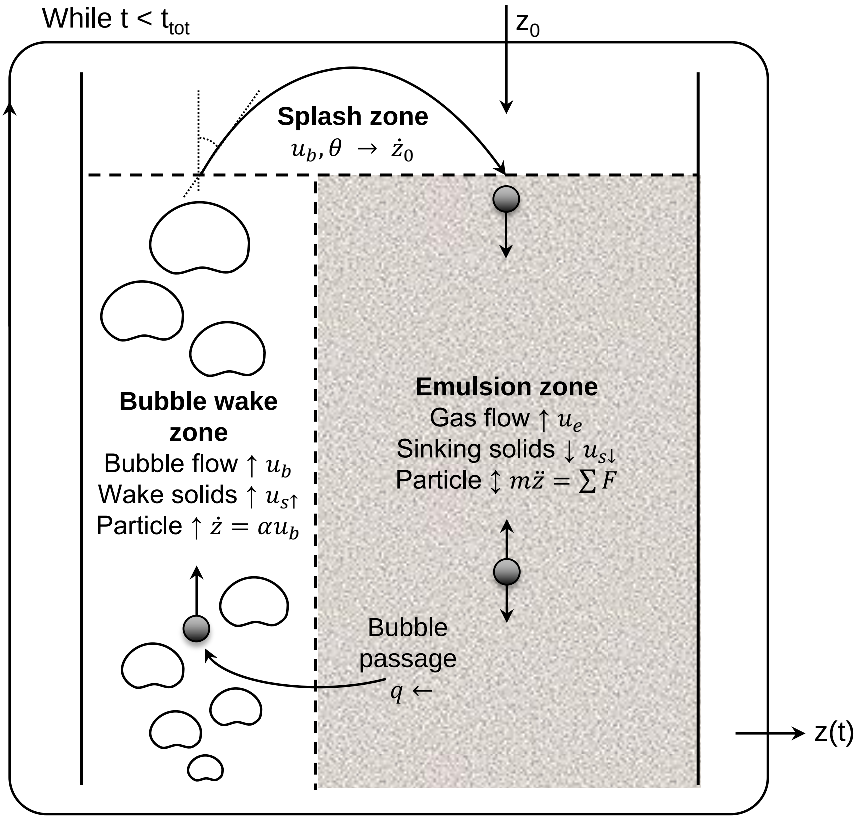
While $t < t_{tot}$
z_0
Splash zone
$u_b, \theta \rightarrow \dot{z}_0$
Bubble wake zone
Bubble flow ↑ u_b
Wake solids ↑ $u_{s\uparrow}$
Particle ↑ $\dot{z} = \alpha u_b$
Emulsion zone
Gas flow ↑ u_e
Sinking solids ↓ $u_{s\downarrow}$
Particle ↕ $m\ddot{z} = \sum F$
Bubble passage
$q \leftarrow$
z(t)

Figure 2.1: Schematic of the Lagrangian model used.

In the emulsion zone, the acceleration of the tracer is calculated according to a balance of the forces acting on the particle: gravitation, buoyancy, drag and lift from gas release from the converting particle.

$$m_p a_p = F_G + F_B + F_D + F_L \tag{3}$$

The buoyancy force is dependent upon the density of the emulsion phase, Eq. (1), while the drag force depends on the viscosity of the bed and the velocity of the sinking bulk particles. This downwards velocity of the solids, $u_{s\downarrow}$, results from the mass balance of the bed material, in which the velocity of the sinking solids compensates for the rising wake solids:

$$u_{s\downarrow} = \frac{f_w \cdot \delta \cdot u_b}{(1-\delta-f_w\delta)} \tag{4}$$

where f_w is the volume fraction of the bubble wake in respect to the bubble volume [18], and δ is the volume fraction of the bubble phase in the dense bed.

In the bubble phase, the tracer particle rises with a fraction, α, of the bubble velocity. The velocity of the bubble flow, u_b, is the sum of the velocity of a single bubble in an infinitely large bed, $u_{br\infty}$ (first term, right-hand side in Eq. (5), expressed according to [37]) and the superficial gas velocity corresponding to the bubble flow, i.e., u_o- u_{mf}- u_{tr}.

$$u_b = 0.711 \cdot \sqrt{g \cdot D_b} + u_o - u_{mf} - u_{tr} \tag{5}$$

When entering the splash zone, the vertical velocity of the tracer is decided by the bubble velocity and an angle, θ, which is taken from experiments [38]. In the splash zone, the particle follows a ballistic movement and re-enters the emulsion zone once it lands back on the dense bed surface.

The model is run for a sufficiently long time to ensure robust statistical significance.

3 Experimental Work

All the experimental work presented in this thesis for Papers I–IV was carried out in one fluid-dynamically down-scaled bubbling fluidised bed (of square cross-section, 0.17×0.17 m^2) using magnetic particle tracking of a single tracer. Figure 3.1 shows the FB unit with one AMR sensor in the foreground.

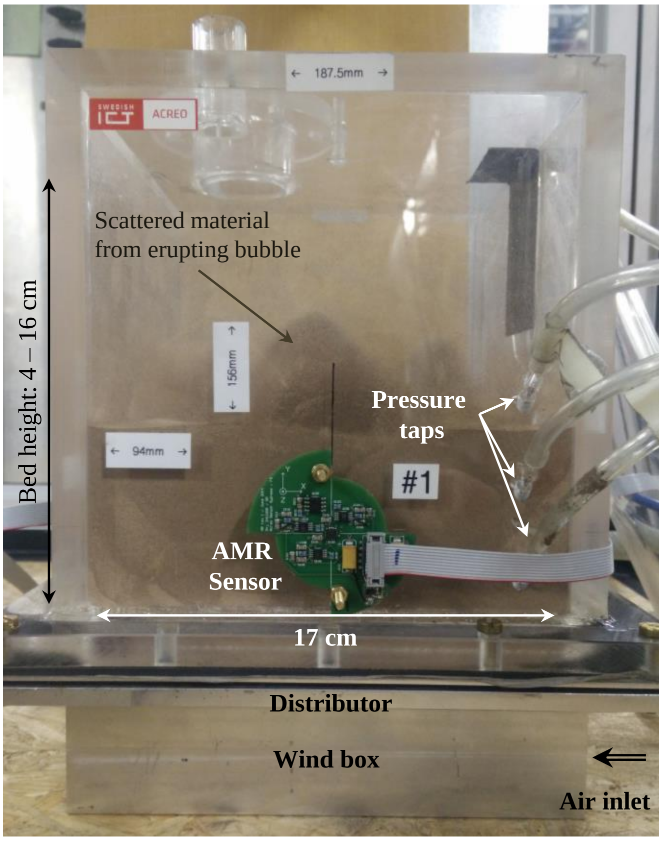
← 187.5mm →
SWEDISH ICT ACREO
Scattered material from erupting bubble
Bed height: 4 – 16 cm
156mm
94mm
Pressure taps
#1
AMR Sensor
17 cm
Distributor
Wind box
Air inlet

Figure 3.1: Experimental set-up. Fluid-dynamically down-scaled bubbling fluidised bed with one AMR sensor in the foreground.

3.1 Fluid-dynamically down-scaled fluidised bed

The bed used is fluid-dynamically down-scaled from an arbitrary bed with bed material typically used in industrial scale beds using the full set of Glicksman's scaling laws [39], which allows for fluid-dynamical investigations at ambient temperature and pressure and is more operationally flexible than large units operated under hot conditions. Thanks to the scaling laws, the data from such cold flow models have quantitative relevance for hot large-scale units and can be applied to investigate, for example, fuel mixing, as shown by Sette et al. [40]. The unit used for the work in Papers II–III was fluidised with air at room temperature and atmospheric pressure, so that up-scaling to different hot conditions (i.e., temperatures, fluidising gas) resulted in different scaling factors.

Table 3.1 summarises the different scaling sets applied in Papers II and III, which resulted in the use as the bed material a bronze powder with a mean particle diameter of 60 µm and a solid density of 8,900 kg/m^3. Paper II used a cylindrical tracer, a permanent magnet of fixed density. For the magnet to resemble an anthracite particle, combustion conditions with a temperature of 900°C were chosen, which resulted in a length scale factor of 5. With further development of the MPT method, Paper III applied three capsulated spherical tracers of constant size but of varying density, resulting in the choice of the more common combustion temperature of 800°C. Both papers apply different bed heights and fluidisation velocities. Papers II and III use a total of four different perforated plates with varying pressure drop characteristics for air distribution.

Table 3.1: Scaling set used in the different papers attached to this work.

	Units	Cold down-scaled	Hot large-scale Paper II (Combustion)	Hot large-scale Paper III (Combustion)
Length scaling	-	*L*	*5 L*	*4.4 L*
Velocity scaling	-	*u*	$\sqrt{5} \cdot u$	$\sqrt{4.4} \cdot u$
Time scaling	-	*t*	$\sqrt{5} \cdot t$	$\sqrt{4.4} \cdot t$
Bed dimensions	m	0.17×0.17	0.85×0.85	0.74×0.74
Bulk solids size	µm	60	300	250
Bulk solids density	kg/m^3	8,900	2,600	2,600
Min. fluid velocity	m/s	0.03	0.07	0.06
Fuel particle (diameter/length)	mm	6/3, 10	15/30	44
Fuel particle density	kg/m^3	1,470–7,310	1,890	350, 800, 1,230
Temperature	°C	20	900	800

3.2 Magnetic particle tracking

All the measurements in Papers II–IV were carried out by means of MPT, which has been shown to be a suitable method for the continuous three-dimensional tracking of an individual tracer particle in fluid-dynamically down-scaled FBs. In such units, the metallic bed material imposes severe limitations on the usage of tomographic methods, while optical methods are limited to the bed surface, as is the case for any three-dimensional unit (see Paper II).

In this thesis, four sensor assemblies were used to track a single tracer particle that consisted of an NdFeB-based permanent magnet. One sensor assembly is mounted on each of the side walls of the bed at a height of 45 mm and contains a three-axis Anisotropic Magneto Resistive (AMR) sensor, which is powered by an external voltage source. The AMR sensor is produced with a default direction, which will change in response to an approaching magnetic field, thereby affecting the electrical resistance of the sensor. Five variables are unknown in this system:

the position (x, y, z) and rotation (φ, θ) of the tracer. With four sets of three-axis sensors, a total of 12 measurements is collected at each sampling point, resulting in an over-determined system, which is solved by minimising the squared difference between the modelled and measured magnetic field. Noise that originates from magnetic fields surrounding the measurement device can be subtracted in the data analysis by taking a background measurement before each experiment.

The magnetic field range of the sensors is ±0.6 mT, which can be exceeded when the magnetic tracer is located close to the sensing elements. Once saturated, the sensor can be restored with magnetisation by sending two short electric pulses, so-called set/reset (S/R) pulses, to the sensor. As sensor saturation is not easily detectable, S/R is performed synchronously with the sampling frequency to ensure that all the sensor elements are measuring properly. However, with this procedure, the sampling frequency is restricted to around 20 Hz, as restoration of a sensing element by an S/R pulse requires the corresponding time.

Paper II presents a solution to the sensor restoration issue based on enabling asynchronous S/R pulses while measuring, thereby yielding higher sampling frequencies (up to 200 Hz). Furthermore, a method to detect and remove measurement data from saturated sensors was developed. In Paper III, tracers with stronger magnetic fields were used, such that the sensor elements were moved further away from the bed wall to minimise sensor saturation. As the magnetic fields of the tracers were stronger, this did not result in a reduction of the signal strength. In addition, the modelled magnetic field implemented in the code that solves the minimisation problem was modified in order to allow for tracers of different magnetic strength to be used.

3.3 Falling sphere experiments

As the work in Paper IV investigates the apparent viscosity of a gas-solids emulsion with non-scaled solids, no fluid-dynamic scaling was applied and Ballotini particles (with a narrow particle size distribution of 212 µm to 250 µm and a solid density of 2,600 kg/m^3) were used as the bed material. The bed was fluidised to the minimum fluidisation conditions (0.048 m/s) with a high bed (13–16 cm), to ensure that the tracer reached its terminal falling velocity. For a smooth fluidisation, a porous plate with a high-pressure drop was used as the air distributor. Furthermore, eight different spherical tracers with sizes in the range of 5–20 mm and densities in the range of 4,340–7,500 kg/m^3 were used in the tests.

4 Results and Discussion

This section summarises the main findings of this thesis by presenting selected results that underline the connections visualised in Figure 1.3. Initially, results showing how the modelling and the experimental work support each other are presented (i.e., horizontal connections in Figure 1.3). Thereafter, results from both the modelling and the experimental work are presented that expand the current understanding of axial mixing (i.e., vertical arrows in Figure 1.3).

4.1 Combination of modelling and experimental work

As discussed in Section 1.2 and indicated in Section 2, this work focuses on four mechanisms (each with a key parameter to be investigated experimentally) that potentially govern the circulation of a tracer particle immersed in a dense bed. They are briefly listed here, and the main findings are presented below:

a) The drag from the sinking bed material acting on the tracer particle (governed by the apparent viscosity of the bed emulsion).
b) The transition of the tracer particle from the emulsion zone with sinking solids to the bubble wake zone (governed by the probability of the particle to join the wake of a passing bubble).
c) The drag of the rising bubble wake acting on the tracer particle (governed by the effective rise velocity of the bubble path).
d) The transition of the tracer particle from the bubble wake zone to the emulsion zone (governed by the probability to detach from a bubble wake and slip back into the emulsion zone with sinking solids).

Transition from bubble wake zone to emulsion zone

The mechanism underlying the transition from the bubble wake zone to the emulsion zone inside the dense bed was studied by evaluating the experimental data acquired for Paper III. Characterized by low measured probabilities for this phase change to occur, the mechanism was found to play a negligible role in the axial mixing of the tracers that mimic tracer particles and was therefore not considered in the modelling. Instead, this zone change was considered to occur exclusively through ejection of the rising fuel particle into the splash zone so that it lands on the dense bed surface of the emulsion zone.

Drag of solids in rising bubble wake on tracer particle

The tracer rise in the bubble wake is considered by assuming that the rise velocity is a fraction of the bubble velocity, α, which reflects that the fuel particles are typically not dragged up in only one wake region, but instead through consecutively joining and detaching from different wake regions. Previously, this fraction was shown to represent 10%–30% of the bubble velocity [24], [27], [41]–[43]. However, the analysis of experimental data related to the investigations described in Paper III reveals the values in literature underestimate the rising velocity of the tracer, hence, α is higher in hot industrial scale units. Additionally, the data showed, that α decreases with increasing fluidisation velocity. Thus, the model in Paper I uses the values obtained from the experiments in Paper III ranging from 94%–55%. Finally, the modelling studies disclose that low α-values (approx. below 15%) result in a significantly different axial tracer particle distribution.

Transition from emulsion zone to bubble wake zone

The probability of the particle to transfer from the sinking emulsion by joining the rising wake solids, q, is a key component of the model presented in Paper I, as it couples the two zones considered in the dense bed and is needed to enable circulation (sinking/rising) of the tracer particle. The q-values were extracted from the (extended) measurement data in Paper III. Figure 4.1 shows the probability over height in the bed of a spherical tracer diameter, 10 mm; solid density, 4,320 kg/m^3) for increasing fluidisation velocity (0.06–0.26 m/s); both the measurement points and fitted curves are plotted and the fixed bed height is indicated in the figure. The probability to join the wake region of a passing bubble is higher in the bottom regions of the dense bed and decreases towards the dense bed surface, where vigorous movement might prevent the tracer from attaching to the rising wake solids. With increasing fluidisation velocity, the probability increases, which is in line with larger bubbles being formed at higher velocities.

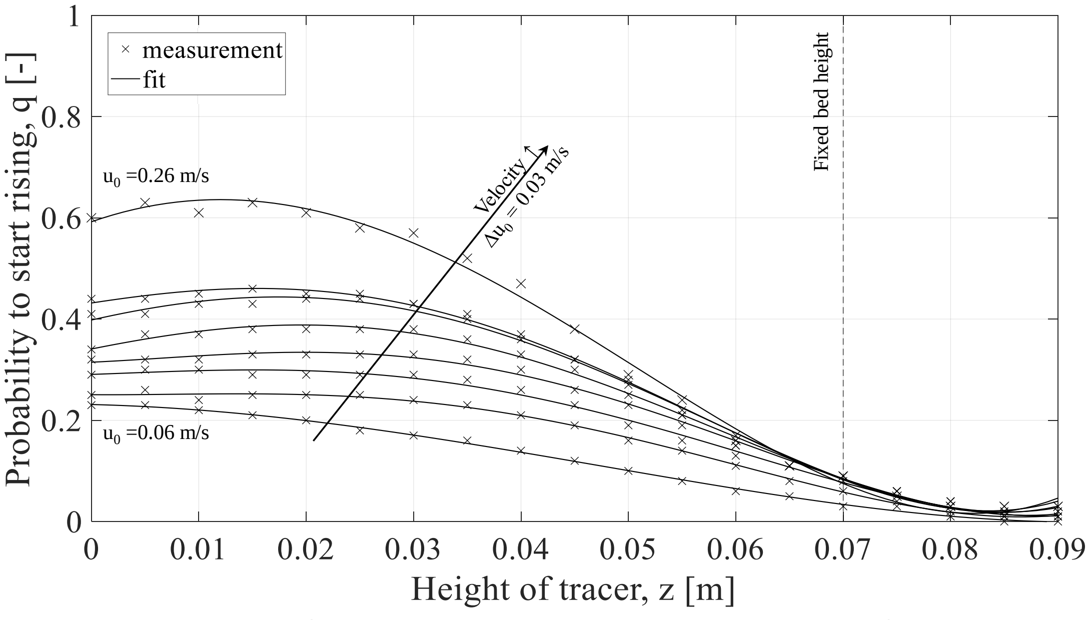

Figure 4.1: Probability of the tracer particle to join the wake region of a bubble, q, over height, z, for different fluidisation velocities (0.06–0.26 m/s). Source: Paper I.

Figure 4.2 shows the mean probability that the tracer will exit the sinking emulsion and join the bubble wake as a function of fluidisation velocity, for different tracer sizes and densities. For all the tracers, the fluidisation velocity increases the probability, albeit to different extents. There is no clear trend regarding the influences of tracer size and density. A possible explanation for this is the flotsam behaviours of these tracers, which makes it difficult to gather measurement points with sufficient representability inside the dense bed. Paper I discuss the further usage in the model of a probability value that is averaged over the dense bed height and for all fluidisation velocities, particles densities and sizes, considering the indefinite influences of tracer size and density in the experiments, as well as the weak influences of variations in this variable on the modelling results.

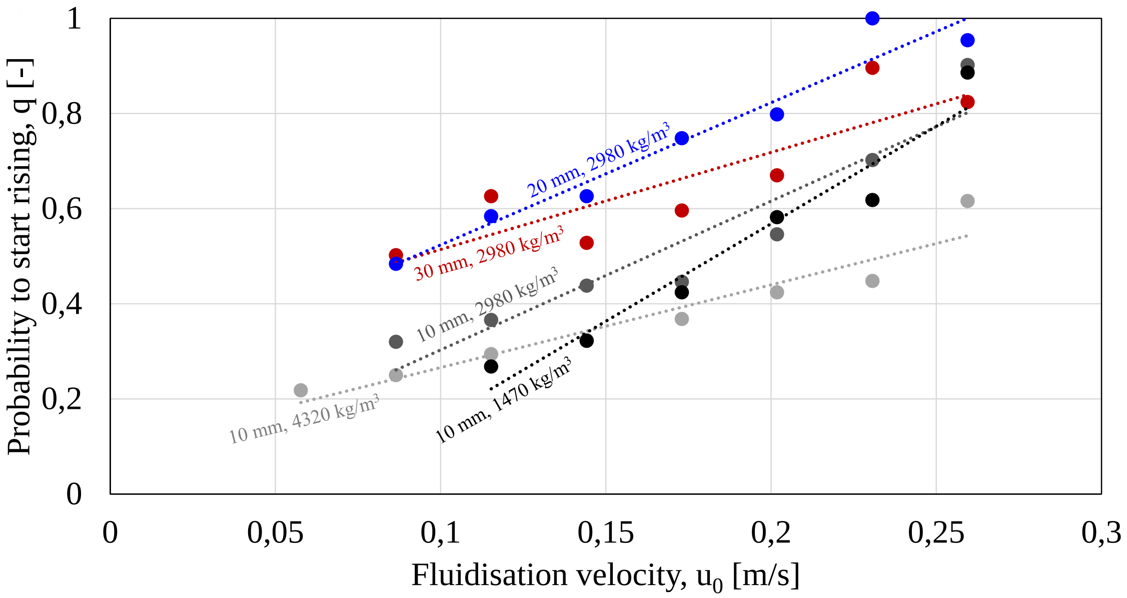

Figure 4.2: Mean probability to start rising, q, over fluidisation velocities, u_0, for different tracer sizes and densities. Source: Extended measurement data from Paper III

Drag of sinking solids on tracer particle

Regarding the drag of the bed material on the tracer particle, in a first version of the model (Paper 2 in the list of *Publications not included in this thesis*), a simple correlation derived from experimental data for one of the tracers in Paper III and which depended exclusively on the velocity difference of the particle to the bed material was used to describe the drag coefficient. This approach was very limited, as it excluded the influence of fuel size, which in Paper III is confirmed to play a key role in axial mixing. Furthermore, as discussed in Paper IV, the models and values described in the literature for the apparent viscosity of the bed were found to be scarce and partly contradictory [35].

Paper IV presents experiments to measure the apparent viscosity of the emulsion of a bed at minimum fluidisation. Figure 4.3 compares the experimental values obtained in Paper IV with values calculated as proposed by Rees et al. [35], who used measurement data from Daniels et al. [31] and who suggested the influence of a defluidised hood that builds up above the sinking tracer and eventually detaches from it, while the viscosity remains constant with changes in the terminal velocity. The measured value of 0.24 Pa s fits well with the values obtained by Rees et al. [35] assuming the defluidised hood to detach as the tracers fall with high terminal velocity. The value of the apparent viscosity in Paper IV is lower as spherical Ballotini particles where used as bed material, while Daniels et al. [31] used sharp sand particles resulting in a higher drag on the tracer particle.

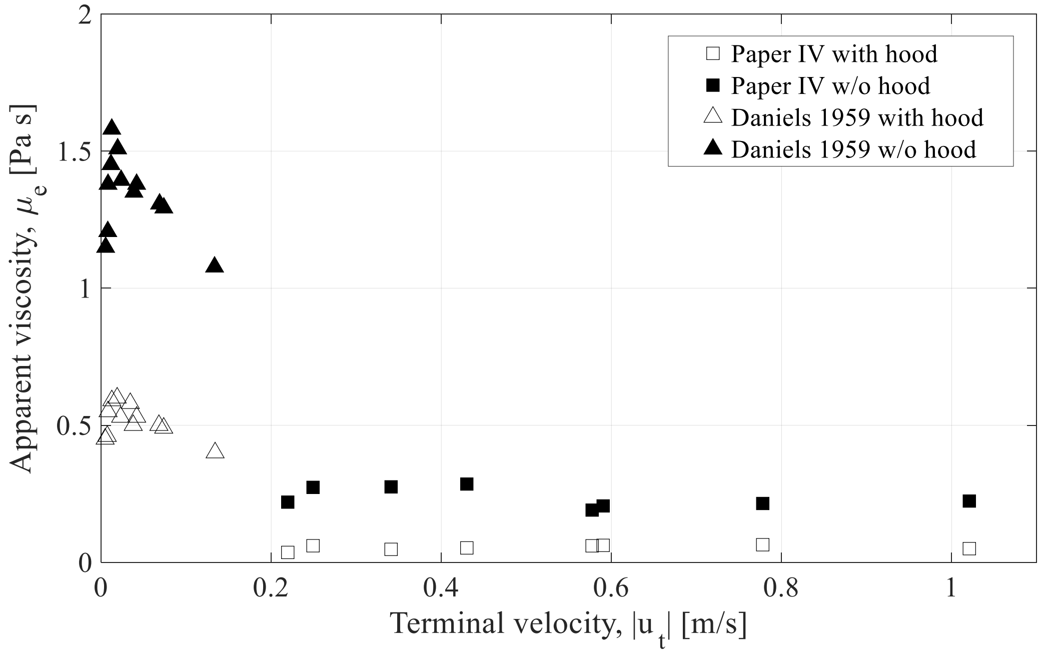

Figure 4.3: Apparent viscosity, μ_e, against the absolute terminal velocity, $|u_t|$. Viscosity is calculated from experiments assuming the presence or absence of a defluidised hood, as proposed by Rees et al. [35]. *Data from this work and Daniels* [31]. *Source: Paper IV.*

The conclusions in Paper IV suggest the usage of a constant apparent viscosity for the gas-solids emulsion in the model described in Paper I and confirm the Newtonian character of the bed emulsion. The measurement range presented in literature [35] is extended with higher terminal velocities, i.e. beyond the linear flow regime. The comparison with the experimental bed viscosity values in the literature obtained with other methods [32], [44], indicates that the measurement method used for spheres at externally controlled velocities (instead of free falling) is intrusive, influencing the drag of the emulsion on the tracer and, therefore, the result of the apparent viscosity.

Furthermore, the model in Paper I was used to evaluate the effect of the viscosity on the circulation of the tracer particle, showing with increased apparent viscosity most observations of the tracer particle are made inside the dense bed. For the model in Paper I the value of 1.24 Pa s was used (as suggested by Rees et al. [35] but up-scaled).

4.2 Axial mixing of large solids

The influences of fluidisation velocity and tracer density on the axial mixing are depicted in Figure 4.4, which compares the modelled (Paper I) and experimental (Paper III) probability density functions (PDF) for the axial location of two different tracer particle densities (810 and 400 kg/m^3). The experiments were conducted as described in Section 3.1 with a bed height of 0.3 m and with two different fluidisation velocities (0.13 and 0.43 m/s). The model used the same input values as well as an α-value for the respective velocities retrieved from experiments in Paper III and an apparent viscosity of 1.24 Pa s. By minimising the squared error for varying the wake volume fraction of the rising bubbles, a value for the wake fraction, f_w, of 0.94 was obtained.

There is good agreement between the modelled and measured data. The model reproduces the trends observed in the experiments, i.e., increasing the fluidisation velocity results in better mixing and lighter particles are more prone to float on the bed surface.

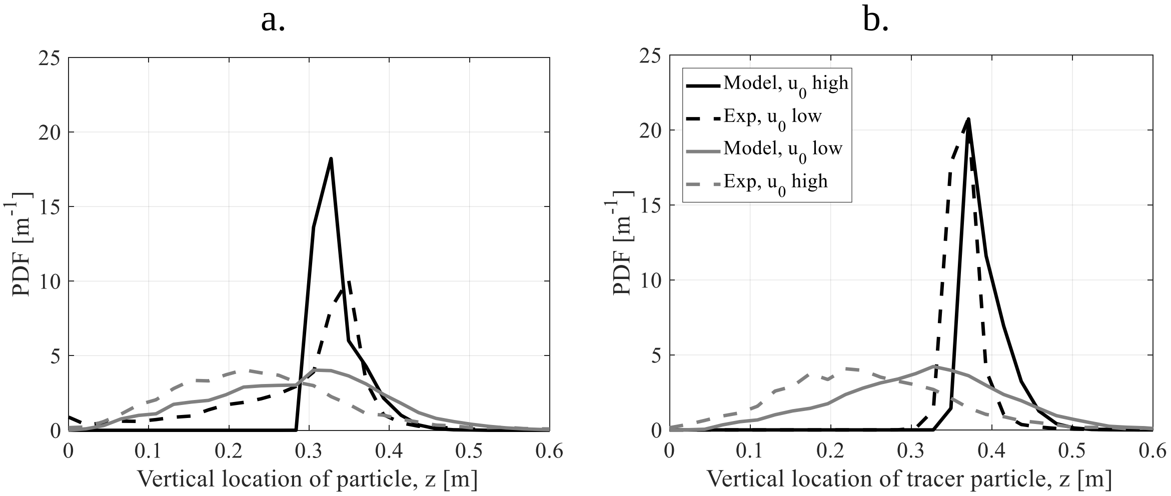

Figure 4.4: Modelled and measured vertical locations of the tracer particle, z, at low and high fluidisation velocities (0.13 m/s and 0.43 m/s). a) Particle density resembling a fresh biomass particle (810 kg/m^3). b) Particle density resembling the remaining biochar (400 kg/m^3). Source: Paper I

The influence of the pressure drop across the gas distributor is shown in Figure 4.5, which compares the spatial distributions of the tracer particle for air distributors with two different pressure drops (Paper II). The tracer particle is more evenly distributed (both laterally and axially) when using a distributor with a higher pressure drop. A low pressure drop enhances the defluidised zones in which the tracer gets trapped for longer periods.

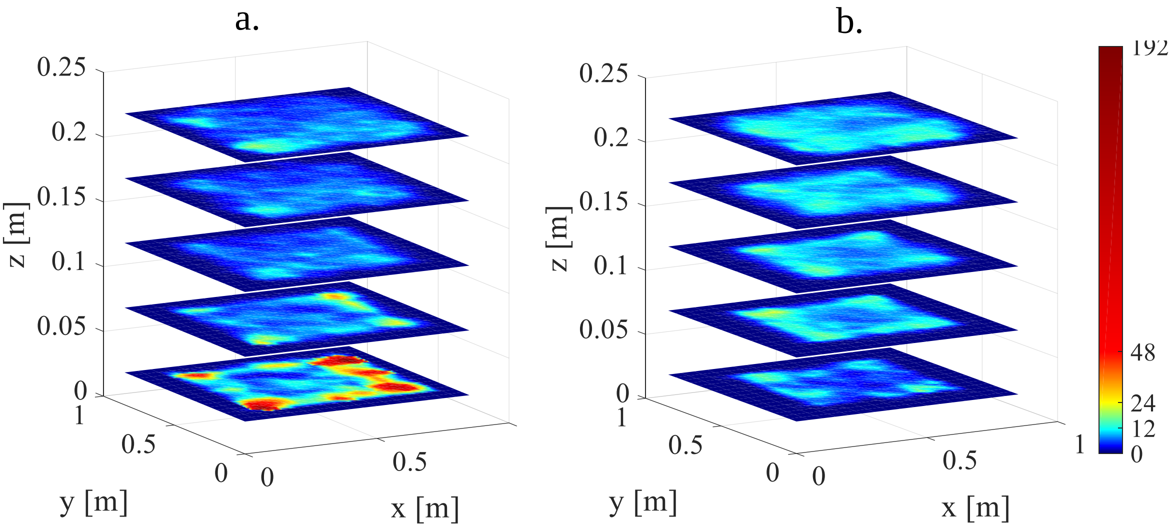

Figure 4.5: Measured spatial distributions of the tracer particle. H_b = 0.25 m; u_0 = 0.22 m/s. a) Low-pressure distributor. b) High-pressure distributor. Note the modified scale in the colour map. Source: Paper II

The flow structure of the tracer is exemplified in Figure 4.6, which shows the data for a vertical slice of the bed (Paper II). The colours indicate the magnitude and direction (up/downwards) of the vertical velocity.

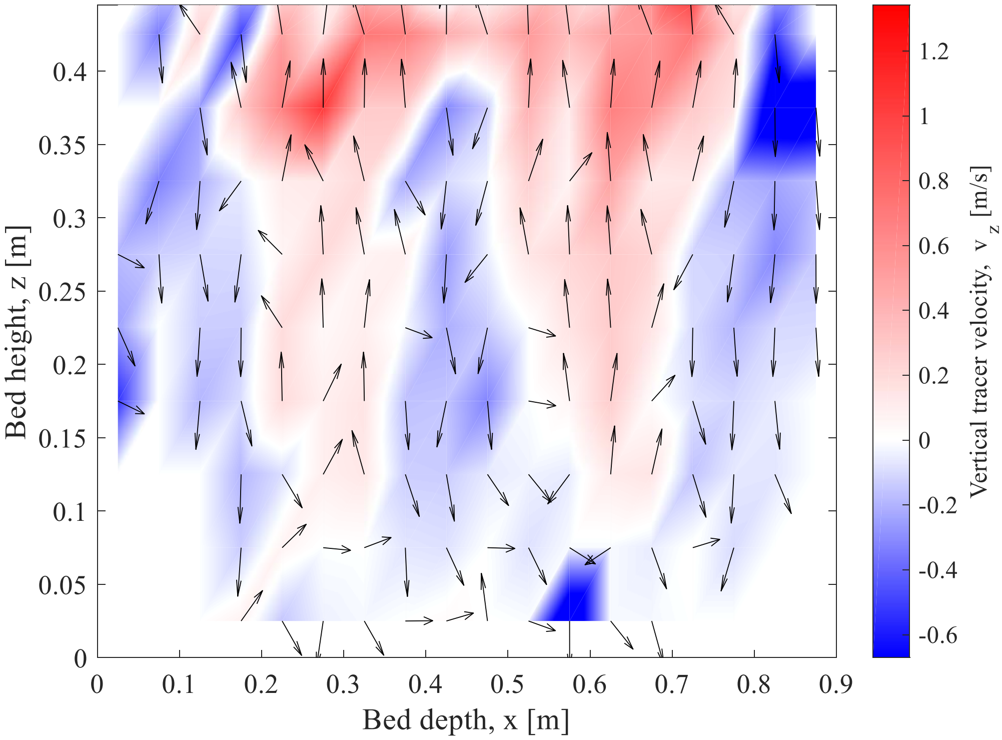

Figure 4.6: Tracer flow structures in a vertical slice located at y = 0.1 m. The background colour indicates the magnitude of the vertical velocity. Low-pressure distributor. H_b = 0.35 m. u_0 = 0.29 m/s. Source: Paper II

In the graph, the dominating bubble paths can be clearly identified at around *x*=0.25 m and *x*=0.65 m. The tracer rises rapidly with the bubble paths and sinks at lower velocities beside and between the paths.

Finally, the segregating tendency of the fuel was studied through the share of time spent by the tracer on and above the dense bed surface. Figure 4.7 plots the share of time against the fluidisation velocity and compares the results from the modelling (Paper I) and experiments (Paper III) for two different tracer densities. The location of the dense bed surface was taken from experiments with a fully flotsam tracer. Three mixing regimes can be identified for typical fuel particles (i.e., with a density lower than that of the gas-solids emulsion): 1) a purely flotsam regime that occurs at low fluidisation velocities; 2) a transition regime in which an increase in fluidisation velocity results in a rapid decrease in the number of observations of the tracer particle at the bed surface; and 3) a stationary regime in which the presence of a tracer particle at the bed surface and in the splash zone remains constant with fluidisation velocity. The onset fluidisation velocities between the regimes depend mainly on the bed height and tracer properties.

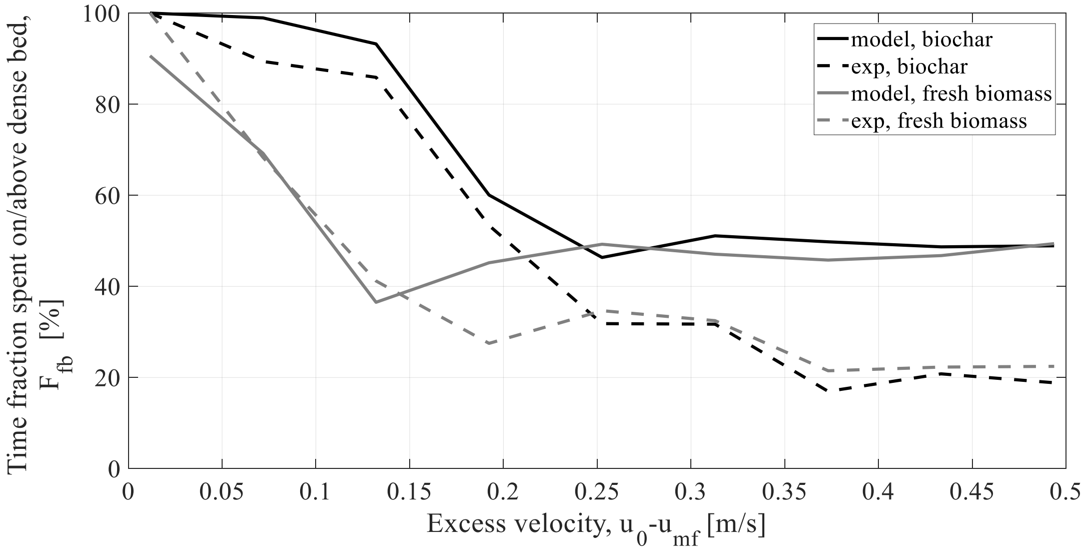

Figure 4.7: Modelled and measured share of time spent on and above the dense bed surface of the tracer particle, F_{fb}, vs. fluidisation velocity, u0-umf. Comparing two tracer densities: fresh biomass (810 kg/m^3) and biochar (400 kg/m^3). Source: Paper I

5 Conclusions

A combination of modelling and experimental work yields an improved understanding of the core mechanisms and connected parameters governing the axial mixing of large solids in the bottom region of fluidised bed units. Experimental work supports the modelling by providing empirical inputs obtained from dedicated experiments, while appropriate use of the model identifies the key knowledge gaps that need to be investigated experimentally.

The apparent viscosity of the emulsion was by means of model investigations found to play an important role for the immersion of fuel particles in a fluidised bed. Dedicated experiments were able to determine the Newtonian character of the bed emulsion and explain contradicting claims provided in previous literature.

Furthermore, the model investigations revealed the importance of a proper description of the bubble flow, more precisely, its influence on both the upwards velocity of the tracer in the bubble wake and the downwards velocity of the sinking bed solids. Experimental work combining fluid-dynamical scaling and magnetic particle tracking (MPT) shows that the previous studies in which the temperature effect was not considered tended to under-estimate the bubble velocity, i.e., literature correlations derived from non-scaled cold laboratory tests are not able to properly describe the bubble flows of large-scale FB units operating under hot conditions.

The axial mixing of large solids can be mathematically described, showing good agreement with the measurements, using a semi-empirical model. The model is based on the definition of two solids zones in the dense bed and one in the splash zone, each with its own flow pattern for the tracer particle. Of these three zones, the mixing in the emulsion zone of the dense bed has the strongest impact on the final axial distribution of the fuel. In this critical phase, the mixing can be satisfactorily described by a balance of forces considering, besides gravity, the buoyancy towards the bed emulsion and the drag force from the sinking bed material.

MPT has been shown to be a suitable method to investigate fuel mixing in fluid-dynamically down-scaled units, providing 3-dimensional distributions of tracer locations and velocities with very high temporal (kHz) and spatial (mm) resolutions. Experimentally, three mixing regimes were identified to characterise in general terms the axial mixing of larger and lighter solids as fluidisation velocity is increased: 1) a purely flotsam regime dominated by the buoyancy force; 2) a transition regime in which the fuel gradually increases the penetration into the dense bed; and 3) a stationary regime in which the drag and buoyancy forces balancing each other and in which the increased fluidisation velocity does not contribute to increased axial mixing of the fuel. It was found that the threshold values of the fluidisation velocity that determine the regime shifts depend on several variables, which have to be determined through modelling.

6 Future research

The main experiments presented in this work were done with spherical tracer particles, although real fuel particles come with a variety of shapes. As MPT is able to provide the orientation of its tracer, the method allows for studying the influence of the shape of non-spherical tracers on the drag force acting on a tracer immersed in the dense bed. However, the cylindrical tracer used in Paper II was observed not to orient with its minimum projected area towards the flow, as expected, but showed a statistically preferred orientation towards the magnetic field of the Earth. To still be able to study the influence of tracer shape, the experiments must be conducted in absence of net external magnetic field, e.g. a Helmholtz field opposing the Earth's magnetic field can be used.

MPT measurements of the falling sphere experiments have so far been limited to the use of glass particles as bed material. However, the importance of the apparent viscosity of the bed emulsion and the scarce data for it available in literature indicate a need for further investigation involving different bed materials (size, density, sphericity, surface rugosity) and conditions (cold, down-scaled from hot conditions).

Notation

Roman letters

A_0	Bubble catchment area, m^2
C_d	Drag coefficient, -
D	Diameter, m
f_2	Empirical expression, -
F_{lift}	Lift force, N
f_w	Bubble wake fraction, -
g	Gravitational constant, m/s^2
H_0	Fixed bed height, m
m	Mass of fuel particle, kg
Q	Released gas flow rate, m^3/s
q	Probability to start rising, %
t	Time, s
u	Velocity, m/s
z	Axial position, m

Greek letters

α	Fuel-to-bubble velocity ratio, -
δ	Bubble fraction, -
θ	Ejection angle, °
μ_0	Apparent viscosity, Pa s
ρ	Density, kg/m^3
τ_{vol}	Devolatilisation time, s

Indices

b	Bubble
br	Single bubble
e	Emulsion
im	Immersion
mf	Minimum fluidisation
o	Initial
p	Fuel particle
s	Solids
tr	Throughflow

References

[1] J. Chaouki and J. Shabanian, “Editorial:Fluidization for Emerging Green Technologies,” *Powder Technol.*, vol. 316, pp. 1–2, Jul. 2017.

[2] K. Dasgupta, J. B. Joshi, and S. Banerjee, “Fluidized bed synthesis of carbon nanotubes – A review,” *Chem. Eng. J.*, vol. 171, no. 3, pp. 841–869, Jul. 2011.

[3] T. Mattisson *et al.*, “Chemical-looping technologies using circulating fluidized bed systems: Status of development,” *Fuel Process. Technol.*, vol. 172, pp. 1–12, Apr. 2018.

[4] M. Nikku, K. Myöhänen, J. Ritvanen, T. Hyppänen, and M. Lyytikäinen, “Three-dimensional modeling of biomass fuel flow in a circulating fluidized bed furnace with an experimentally derived momentum exchange model,” *Chem. Eng. Res. Des.*, vol. 115, pp. 77–90, 2016.

[5] C. T. Crowe, J. D. Schwarzkopf, M. Sommerfeld, and Y. Tsuji, *Multiphase Flows with Droplets and Particles*, Second Edi. 2011.

[6] D. Pallarès and F. Johnsson, “Modeling of fuel mixing in fluidized bed combustors,” *Chem. Eng. Sci.*, vol. 63, no. 23, pp. 5663–5671, 2008.

[7] L. Ratschow, R. Wischnewski, E. U. Hartge, and J. Werther, “Three-Dimensional Simulation of Temperature Distributions in Large-Scale Circulating Fluidized Bed Combustors,” in *Proceedings of the 20th International Conference on Fluidized Bed Combustion*, 2010, pp. 780–785.

[8] K. Myöhänen and T. Hyppänen, “A Three-Dimensional Model Frame for Modelling Combustion and Gasification in Circulating Fluidized Bed Furnaces,” *International Journal of Chemical Reactor Engineering*, vol. 9. 2011.

[9] J. Koornneef, M. Junginger, and A. Faaij, “Development of fluidized bed combustion—An overview of trends, performance and cost,” *Prog. Energy Combust. Sci.*, vol. 33, no. 1, pp. 19–55, 2007.

[10] K. Qin, H. Thunman, and B. Leckner, “Mass transfer under segregation conditions in fluidized beds,” *Fuel*, vol. 195, pp. 105–112, 2017.

[11] L. Lundberg, P. A. Tchoffor, D. Pallarès, R. Johansson, H. Thunman, and K. Davidsson, “Influence of surrounding conditions and fuel size on the gasification rate of biomass char in a fluidized bed,” *Fuel Process. Technol.*, vol. 144, pp. 323–333, 2016.

[12] J. Olsson, D. Pallarès, and F. Johnsson, “Lateral fuel dispersion in a large-scale bubbling fluidized bed,” *Chem. Eng. Sci.*, vol. 74, no. 0, pp. 148–159, 2012.

[13] A. Svensson, F. Johnsson, and B. Leckner, “Bottom bed regimes in a circulating fluidized bed boiler,” *Int. J. Multiph. Flow,* vol. 22, no. 6, pp. 1187–1204, 1996.

[14] D. Kunii and O. Levenspiel, *Fluidization Engineering*. Butterworth-Heinemann, 1991.

[15] J. F. Davidson and D. Harrison, “Fluidised particles,” vol. First Brit. Cambridge University Press, New York, 1963.

[16] P. N. Rowe, B. A. Partridge, A. G. Cheney, G. A. Henwood, and E. Lyall, “The mechanisms of solids mixing in fluidised beds,” *Chem. Eng. Res. Des.*, vol. 43a, pp. 271–286, 1965.

[17] I. N. M. Woollard and O. E. Potter, “Solids mixing in fluidized beds,” *AIChE J.*, vol. 14, no. 3, pp. 388–391, May 1968.

[18] P. N. Rowe and B. A. Partridge, “An x-ray study of bubbles in fluidised beds,” *Chem. Eng. Res. Des.*, vol. 75, Supple, no. 0, pp. S116–S134, 1997.

[19] I. Eames and M. A. Gilbertson, “Mixing and drift in gas-fluidised beds,” *Powder Technol.*, vol. 154, no. 2–3, pp. 185–193, 2005.

[20] Y. Shi and L. T. Fan, “Lateral mixing of solids in batch gas-solids fluidized beds,” *Ind. Eng. Chem. Process Des. Dev.*, vol. 23, no. 2, pp. 337–341, 1984.

[21] J. R. Grace and R. Clift, “On the two-phase theory of fluidization,” *Chem. Eng. Sci.*, vol. 29, no. 2, pp. 327–334, 1974.

[22] J. Werther, “Bubble chains in large diameter gas fluidized beds,” *Int. J. Multiph. Flow,* vol. 3, no. 4, pp. 367–381, 1977.

[23] D. Pallarès and F. Johnsson, “A novel technique for particle tracking in cold 2-dimensional fluidized beds—simulating fuel dispersion,” *Chem. Eng. Sci.*, vol. 61, no. 8, pp. 2710–2720, Apr. 2006.

[24] A. Soria-Verdugo, L. M. Garcia-Gutierrez, S. Sanchez-Delgado, and U. Ruiz-Rivas, “Circulation of an object immersed in a bubbling fluidized bed,” *Chem. Eng. Sci.*, vol. 66, no. 1, pp. 78–87, 2011.

[25] P. N. Rowe, A. W. Nienow, and A. J. Agbim, “The mechanisms by which particles segregate in gas fluidised beds - binary systems of near-spherical particles,” *Trans. Inst. Chem. Eng.*, vol. 50, pp. 310–323, 1972.

[26] P. N. Rowe and A. W. Nienow, “Particle mixing and segregation in gas

fluidised beds. A review," *Powder Technol.*, vol. 15, no. 2, pp. 141–147, Nov. 1976.

[27] A. W. Nienow, P. N. Rowe, and T. Chiwa, "Mixing and segregation of a small proportion of large particles in gas fluidized beds of considerably," *AIChE Symp. Ser.*, vol. 74, pp. 45–53, 1978.

[28] F. Johnsson, S. Andersson, and B. Leckner, "Expansion of a freely bubbling fluidized bed," *Powder Technol.*, vol. 68, no. 2, pp. 117–123, 1991.

[29] J. R. Grace, "The viscosity of fluidized beds," *Can. J. Chem. Eng.*, vol. 48, no. 1, pp. 30–33, Feb. 1970.

[30] K. Schügerl, M. Merz, and F. Fetting, "Rheologische eigenschaften von gasdurchströmten fliessbettsystemen," *Chem. Eng. Sci.*, vol. 15, no. 1–2, pp. 1–38, Jul. 1961.

[31] T. C. Daniels, "Density separation in gaseous fluidized beds," *Rheol. Disperse Syst.*, vol. 5, pp. 211–221, 1959.

[32] T. C. Daniels, "Measurement of the Drag on Spheres Moving through Gaseous Fluidized Beds," *J. Mech. Eng. Sci.*, vol. 4, no. 2, pp. 103–110, 1962.

[33] T. C. Daniels, "Measurement of the drag on immersed bodies in fluidised beds," *Rheol. Acta*, vol. 4, no. 3, pp. 192–197, 1965.

[34] A. C. Rees, J. F. Davidson, J. S. Dennis, and A. N. Hayhurst, "The rise of a buoyant sphere in a gas-fluidized bed," *Chem. Eng. Sci.*, vol. 60, no. 4, pp. 1143–1153, 2005.

[35] A. C. Rees, J. F. Davidson, J. S. Dennis, and A. N. Hayhurst, "The Apparent Viscosity of the Particulate Phase of Bubbling Gas-Fluidized Beds: A Comparison of the Falling or Rising Sphere Technique with Other Methods," *Chem. Eng. Res. Des.*, vol. 85, no. 10, pp. 1341–1347, 2007.

[36] A. Köhler, A. Rasch, D. Pallarès, and F. Johnsson, "Experimental characterization of axial fuel mixing in fluidized beds by magnetic particle tracking," *Powder Technol.*, vol. 316, pp. 492–499, 2017.

[37] R. C. Darton, R. La Nauze, J. F. Davidson, and D. Harrison, "Bubble Growth Due To Coalescence in Fluidized Beds," *Trans. Inst. Chem. Eng.*, vol. 55, pp. 274–280, 1977.

[38] L. M. Garcia-Gutierrez, A. Soria-Verdugo, C. Marugán-Cruz, and U. Ruiz-Rivas, "Simulation and experimental study on the motion of non-reacting objects in the freeboard of a fluidized bed," *Powder Technol.*, vol. 263, pp. 112–120, Sep. 2014.

[39] L. R. Glicksman, M. R. Hyre, and P. A. Farrell, “Dynamic similarity in fluidization,” *Int. J. Multiph. Flow*, vol. 20, no. SUPPL. 1, pp. 331–386, 1994.

[40] E. Sette, D. Pallarès, and F. Johnsson, “Experimental quantification of lateral mixing of fuels in fluid-dynamically down-scaled bubbling fluidized beds,” *Appl. Energy*, vol. 136, no. 0, pp. 671–681, 2014.

[41] G. M. Rios, K. Dang Tran, and H. Masson, “FREE OBJECT MOTION IN A GAS FLUIDIZED BED,” *Chem. Eng. Commun.*, vol. 47, no. 4–6, pp. 247–272, 1986.

[42] K. S. Lim and P. K. Agarwal, “Circulatory motion of a large and lighter sphere in a bubbling fluidized bed of smaller and heavier particles,” *Chem. Eng. Sci.*, vol. 49, no. 3, pp. 421–424, 1994.

[43] A. Soria-Verdugo, L. M. Garcia-Gutierrez, N. García-Hernando, and U. Ruiz-Rivas, “Buoyancy effects on objects moving in a bubbling fluidized bed,” *Chem. Eng. Sci.*, vol. 66, no. 12, pp. 2833–2841, 2011.

[44] T. C. Daniels, “Measurement of the drag on immersed bodies in fluidised beds,” *Rheol. Acta*, vol. 4, no. 3, pp. 192–197, 1965.